

Published in final edited form as:

RSC Adv. 2014 January 1; 4(50): 26487–26490. doi:10.1039/C4RA04765F.

Enzyme-instructed self-assembly of hydrogelators consisting of nucleobases, amino acids, and saccharide

Dan Yuan, Rong Zhou, Junfeng Shi, Xuwen Du, Xinming Li, and Bing Xu*

Department of Chemistry, Brandeis University, 415 South St., Waltham, MA 02453, USA. Fax: 781-736-2516; Tel: 781-736-5201

Abstract

We report the first example of the use of enzymes to trigger the self-assembly of the conjugates of nucleobases, amino acids, and saccharide to form supramolecular hydrogels in water, which illustrates a facile approach for the development of a new class of multifunctional soft materials for biomedical applications.

Nucleobases, amino acids, and saccharide are the fundamental building blocks chosen by nature for constructing nucleic acids, proteins, and carbohydrates, which ultimately leads to the evolution of life.¹ This fact implies that these building blocks are suitable for the development of biomaterials, particularly soft biomaterials. Recognizing the promises of biological building blocks in the development of soft materials, considerable amount of efforts have focused on the use of biological building blocks for generating supramolecular soft materials (e.g., gels and liquid crystals), which already have made considerable progresses.² For example, saccharide-based hydrogels have found applications for thermally controlled release of DNA,³ or sequestering of RNA,⁴ and a colorimetric sensor array chip.⁵ Hydrogels based on β -hairpin scaffold of peptides have exhibited selective inhibition bacterial growth.⁶ Small peptides or even amino acids have resulted in pH-controlled, self-sorting hydrogelators,⁷ a tris-glycine-SDS gel for electrophoresis of proteins,⁸ sensors for the detection of proteases,⁹ an acid sensitive copolymer for drug delivery,¹⁰ and numerous of enzyme-responsive materials.¹¹ Besides as a building block for self-assembly in water,¹² nucleobases form oligomer of DNA to result in unique liquid crystals.¹³

Encouraged by the above-mentioned progresses, we have been developing supramolecular hydrogelators based on the three types of fundamental building blocks of biomacromolecules. We have found that the simple covalent linkage of nucleobase, amino acids, and saccharide^{12c, 14} affords a new class of supramolecular hydrogelators that exhibit multiple functions (e.g., hydrogelation, cell biocompatible, and binding and delivery of nucleic acids^{14a}). The remarkable structural and functional diversities offered by the self-assembling conjugates of nucleobases, amino acids, and saccharide make them attractive

candidates for the further development of this class of supramolecular hydrogels¹⁵ as new soft biomaterials. To serve as a “smart” soft biomaterial, one useful property for the hydrogelators is to self-assemble and to form a hydrogel according biological cue, such as enzymatic transformation. In fact, enzymatic reaction has become a powerful way to control the spatiotemporal profile of supramolecular hydrogels, which has already led to new discoveries, for example, phosphatase catalysed hydrogelation of D-peptides¹⁶ for selective inhibition of cancer cells.¹⁷ Inspired by those works and other exciting development on enzymatic hydrogelation,¹⁸ we choose to investigate the enzyme-instructed self-assembly of the hydrogelators consisting of nucleobase, amino acids, and saccharide since it has yet to be studied despite their promises.

Scheme 1 shows the structures of the conjugates (**1-4**), which all consist of a thymine (as the nucleobase), phenylalanine(s) (as the amino acids), phosphorylated tyrosine (as the enzymatic trigger^{15d} and an amino acid), and D-glucosamine (as the saccharide). After phosphatase-catalysed dephosphorylation, the conjugates transform from the precursors (**1a-4a**) to the hydrogelators (**1b-4b**). The solutions of all precursors, upon the addition of alkaline phosphatase (ALP), are able to turn into the hydrogels of the corresponding hydrogelators (Fig. 1). Due to the structural difference among them, each precursor exhibits the transition at slightly different conditions. For example, **2b** forms a hydrogel after being aged for a relatively long time (8 days), while other compounds are able to form hydrogels in 5 minutes. At the concentration of 1.0 wt%, precursor **3a** self-assembles to form nanofibers and results in hydrogel even without the treatment of ALP. Interestingly, while **1a** and **2a** exhibit similar cell compatibility, the cytotoxicity of **3a** differs drastically from that of **4a**. This result suggests that the judicious choice of the length of the peptide and the chirality of the amino acids in the conjugates, together with enzymatic conversion, is an effective approach to modulate the biological activity of the assemblies of the conjugates for desired applications. As the first case of enzyme-instructed self-assembly and hydrogelation of these molecular conjugates, this work, thus, provide a useful insight for designing molecular conjugates as new soft materials for various biological and biomedical applications.

We choose to design, synthesize, and examine the substrates shown in Scheme 1 according the following rationale: (i) To introduce enzyme-instructed self-assembly, we incorporate phosphorylated tyrosine (_pTyr). (ii) To evaluate intermolecular aromatic–aromatic interactions,¹⁹ we use different numbers of phenylalanine (one or two). (iii) To examine the influence of the chirality of the amino acids, we used L-amino acid residues (for **1** and **3**) and D-amino acid residues (for **2** and **4**). The switch of the chirality of the amino acid residues (but not the chirality of the saccharide) affords two pairs of diastereomers, which allow us to examine the influence of the stereochemistry to the biological activities of this class of conjugates, an intriguing aspect that has yet to be evaluated. To prepare the conjugates (Scheme 1), we first followed the previously reported procedures to make phosphorylated tyrosine.²⁰ Then, by using solid phase peptide synthesis (SPPS), we obtained the nucleopeptides.^{14c} Next, we attached C-terminal of amino acids to D-glucosamine by coupling reagents HBTU and DIEA. Finally, using HPLC to purify the crude products, we obtained **1a**, **2a**, **3a**, and **4a** at 25~31% in total yields.

After the synthesis of the precursors, we tested their transformation to the hydrogelators for enzyme-instructed self-assembly. As shown in Fig. 1, the precursors, **1a-4a**, are transparent solutions in PBS buffer (**1a**, **2a** and **4a** at 1.0 wt%, **3a** at 0.5 wt%). The addition of ALP (12.5 u/mL) removes phosphate group from the precursors and results in the corresponding hydrogelators (**1b-4b**) that are more hydrophobic than their precursors. While all the hydrogelators form the hydrogels, each exhibits its own characteristics. **1b** and **4b** form stable hydrogels in 5 minute, but **2b** requires relative long time of aging to afford a self-support hydrogel. **3b**, at 0.5 wt%, self-assembles to form a hydrogel in two hours. Interesting, **3a** forms a hydrogel at 1.0 wt% (Fig. S2) in one hour, suggesting that there is sufficient intermolecular interactions among **3a** to drive the formation of the network of **3a** (at 1.0 wt%) as the matrices of the hydrogel.

To understand the rheological behaviors of the hydrogels, we compared their profiles of strain sweep and frequency sweep at the hydrogelator concentrations of 1.0 wt% (Fig. 2). Hydrogel of **3b** possesses the highest maximum storage modulus of 6.97×10^3 Pa. Hydrogels of **1b** and **4b** have similar storage moduli of 1.56×10^3 Pa and 1.57×10^3 Pa, respectively. Hydrogel of **2b** exhibits the lowest storage modulus of 1.15×10^3 Pa. These results are consistent with that **2b** requires the longest time for hydrogelation. The critical strains of the hydrogels **1b-4b** differ only slightly and are 0.52, 0.74, 0.52, and 0.58%, respectively, suggesting that hydrogels **1b-4b** exhibit similar properties to resist external force. Frequency sweep (Fig. 3B) shows that storage modulus is always higher than loss modulus for each hydrogel, which is consistent with the viscoelasticity of the hydrogels.

We used transmission electron micrograph (TEM) to evaluate the microstructures of these enzymatically formed hydrogels. Besides the non-fibrillar aggregates and large fiber bundles as the dominated morphology, there are a small fraction of nanofibers with average widths of 6 ± 2 nm in the hydrogel of **1b** (Fig. 3A). Before **2b** self-assembles to form the hydrogel, solution of **2b** has similar morphologies with the hydrogel of **1b**, which comprises of aggregates and nanofibers. After 8 days' aging, the hydrogel of **2b** consists of thin, long, and entangled nanofibers with diameters about 5 ± 1 nm (Fig. 3B). The presence of bundles or non-fibrillar aggregates in Figure 3A, B suggests the polymorphism of the self-assembling of **1b** and **2b**. While the hydrogel of **3b** contains long and flexible nanofibers with average widths of 5 ± 2 nm (Fig. 3C), which largely entangle, the long and rigid nanofibers (with average widths of 7 ± 2 nm) in the hydrogel of **4b** self-assembles to afford bundles (Fig. 3D). Although the detailed correlation between the molecular structures and the morphological differences of the nanostructures in these hydrogels remains to be established, the chirality of amino acids and numbers of phenylalanine in the hydrogelators, obviously, likely play a vital role in their self-assembly in water.

To examine the cytotoxicity of **1a-4a**, we incubated HeLa cells with them at different concentrations for 3 days (Fig. 4). Precursors **1a** and **2a**, which employ one phenylalanine residue, are essentially compatible with cells as the cell viabilities are both around 80 % at 500 μ M for 72 hours (Fig 4A and 4B). However, conjugates **3a** and **4a**, which contain two phenylalanine residues, exhibit remarkable differences in cell compatibility at 500 μ M. As shown in Fig 4C and 4D, precursors **3a** and **4a** hardly inhibit the proliferation of the cells at

the concentrations from 20 μM to 400 μM . But **3a**, at 500 μM , significantly inhibits the proliferation of the HeLa cells (viability less than 10%), while **4a** is slightly cytotoxicity (cell viability about 70 %). More detailed cell viability test in the presence of **3a**, from 100 to 500 μM (Fig. S4A), determines the IC_{50} of **3a** to be $371 \pm 2 \mu\text{M}$ for 72 hours, which is much lower than that of **4a** (higher than 500 μM). The mixing of **3a** and A_{10} (a single-strand deoxyribonucleic acid) to treat HeLa cells (Fig. S4B) hardly affects the efficacy of **3a**, suggesting that there is little interaction between A_{10} and **3a**. TEM of **3a** at 500 μM reveals considerable amount of aggregates (Fig. S5), which likely are responsible for the cytotoxicity of **3a**. Moreover, with the treatment of ALP, **3a** (500 μM) turns to **3b** and affords thin, long and flexible nanofibers with average widths of $4 \pm 1 \text{ nm}$ (Fig. S5D). However, **4a** (at 500 μM) turns to **4b** and still results in aggregates (Fig. S5F). Like **4b**, **1b** self-assembles to form aggregates (Fig. S5B) at 500 μM . Although such morphological differences coincide with the different cytotoxicities, the detailed mechanisms remain to be elucidated.

In summary, we developed a new type of molecular conjugates made of nucleobases, amino acids, and saccharide for enzyme-instructed self-assembly in water. This approach illustrated in this work will allow one to choose candidates from the large pool of peptide epitopes and lectin-binding small saccharides for developing novel soft biomaterials.²¹ Particularly, the drastically different cytotoxicities exhibited by **3a** and **4a** and the recently observed self-assembled pericellular nanonets¹⁷ suggest that one may tailor the cell compatibility of the hydrogelators by switching the chirality of the peptides in the conjugates.

Supplementary Material

Refer to Web version on PubMed Central for supplementary material.

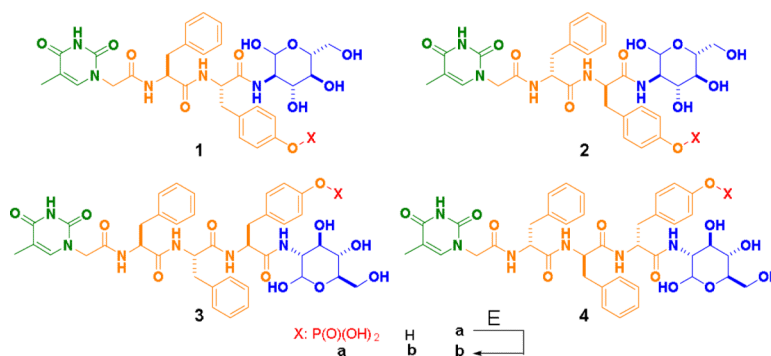
Acknowledgments

This work was partially supported by NIH (R01CA142746) and a Keck grant. We thank the Brandeis EM facility.

Notes and references

1. Mann S. *Angew. Chem. Int. Ed.* 2013; 52:155.
2. a Veiga, A. Salomé; Schneider, JP. *Pept. Sci.* 2013; 100:637. b Cui H, Pashuck ET, Velichko YS, Weigand SJ, Cheatham AG, Newcomb CJ, Stupp SI. *Science.* 2010; 327:555. [PubMed: 20019248] c Numata M, Shinkai S. *Chem. Commun.* 2011; 47:1961. d Babu SS, Praveen VK, Ajayaghosh A. *Chem. Rev.* 2014; 114:1973. [PubMed: 24400783]
3. Kiyonaka S, Sugiyasu K, Shinkai S, Hamachi I. *J. Am. Chem. Soc.* 2002; 124:10954. [PubMed: 12224923]
4. Yang Z, Kuang Y, Li X, Zhou N, Zhang Y, Xu B. *Chem. Commun.* 2012; 48:9257.
5. Ochi R, Kurotani K, Ikeda M, Kiyonaka S, Hamachi I. *Chem. Commun.* 2013; 49:2115.
6. Salick DA, Kretsinger JK, Pochan DJ, Schneider JP. *J. Am. Chem. Soc.* 2007; 129:14793. [PubMed: 17985907]
7. Morris KL, Chen L, Raeburn J, Sellick OR, Cotanda P, Paul A, Griffiths PC, King SM, O'Reilly RK, Serpell LC, Adams DJ. *Nat. Commun.* 2013; 4:1480. [PubMed: 23403581]
8. Yamamichi S, Jinno Y, Haraya N, Oyoshi T, Tomitori H, Kashiwagi K, Yamanaka M. *Chem. Commun.* 2011; 47:10344.

9. Bremmer SC, Chen J, McNeil AJ, Soellner MB. *Chem. Commun.* 2012; 48:5482.
10. Gillies ER, Frechet JMJ. *Chem. Commun.* 2003:1640.
11. Ulijn RV. *J. Mater. Chem.* 2006; 16:2217.
12. a Tan HP, Xiao C, Sun JC, Xiong DS, Hu XH. *Chem. Commun.* 2012; 48:10289. b Shen C, Cramer JR, Jacobsen MF, Liu L, Zhang S, Dong M, Gothelf KV, Besenbacher F. *Chem. Commun.* 2013; 49:508. c Wu D, Zhou J, Shi J, Du X, Xu B. *Chem. Commun.* 2014; 50:1992. d Sessler JL, Jayawickramarajah J. *Chem. Commun.* 2005:1939. e Du X, Li J, Gao Y, Kuang Y, Xu B. *Chem. Commun.* 2012; 48:2098.
13. a Nakata M, Zanchetta G, Chapman BD, Jones CD, Cross JO, Pindak R, Bellini T, Clark NA. *Science.* 2007; 318:1276. [PubMed: 18033877] b Zanchetta G, Nakata M, Buscaglia M, Bellini T, Clark NA. *PNAS.* 2008; 105:1111. [PubMed: 18212117]
14. a Li X, Kuang Y, Shi J, Gao Y, Lin H-C, Xu B. *J. Am. Chem. Soc.* 2011; 133:17513. [PubMed: 21928792] b Li X, Du X, Gao Y, Shi J, Kuang Y, Xu B. *Soft Matter.* 2012; 8:7402. [PubMed: 22844343] c Li XM, Kuang Y, Lin HC, Gao Y, Shi JF, Xu B. *Angew. Chem. Int. Ed.* 2011; 50:9365.
15. a Yang Z, Liang G, Ma M, Abbah AS, Lu WW, Xu B. *Chem. Commun.* 2007:843. b Peng K, Tomatsu I, Kros A. *Chem. Commun.* 2010; 46:4094. c Li X, Gao Y, Kuang Y, Xu B. *Chem. Commun.* 2010; 46:5364. d Yang Z, Liang G, Xu B. *Acc. Chem. Res.* 2008; 41:315. [PubMed: 18205323] e Sangeetha NM, Maitra U. *Chem. Soc. Rev.* 2005; 34:821. [PubMed: 16172672]
16. Li JY, Gao Y, Kuang Y, Shi JF, Du XW, Zhou J, Wang HM, Yang ZM, Xu B. *J. Am. Chem. Soc.* 2013; 135:9907. [PubMed: 23742714]
17. Kuang Y, Shi JF, Li JY, Yuan D, Alberti KA, Xu QB, Xu B. *Angew. Chem. Intl. Ed.* 2014 in press.
18. a Hughes M, Frederix PWJM, Raeburn J, Birchall LS, Sadownik J, Coomer FC, Lin IH, Cussen EJ, Hunt NT, Tuttle T, Webb SJ, Adams DJ, Ulijn RV. *Soft Matter.* 2012; 8:5595. b Bremmer SC, McNeil AJ, Soellner MB. *Chem. Commun.* 2014; 50:1691. c Gao J, Zheng W, Zhang J, Guan D, Yang Z, Kong D, Zhao Q. *Chem. Commun.* 2013; 49:9173. d Zhou J, Du X, Gao Y, Shi J, Xu B. *J. Am. Chem. Soc.* 2014; 136:2970. [PubMed: 24512553]
19. Shi JF, Gao YA, Yang ZM, Xu B. *Beilstein J. Org. Chem.* 2011; 7:167. [PubMed: 21448260]
20. a Alewood PF, Johns RB, Valerio RM, Kemp BE. *Synthesis-Stuttgart.* 1983:30. b Ottinger EA, Shekels LL, Bernlohr DA, Barany G. *Biochemistry.* 1993; 32:4354. [PubMed: 7682846]
21. a He M, Li J, Tan S, Wang R, Zhang Y. *J. Am. Chem. Soc.* 2013; 135:18718. [PubMed: 24106809] b Raeburn J, McDonald TO, Adams DJ. *Chem. Commun.* 2012; 48:9355. c Sadownik JW, Leckie J, Ulijn RV. *Chem. Commun.* 2011; 47:728. d Steed JW. *Chem. Commun.* 2011; 47:1379. e Yan C, Pochan DJ. *Chem. Soc. Rev.* 2010; 39:3528. [PubMed: 20422104] f Matson JB, Stupp SI. *Chem. Commun.* 2012; 48:26.

**Scheme 1.**

Structures of the precursors and the corresponding hydrogelators consist of nucleobase, amino acids, and saccharide. E is a phosphatase.

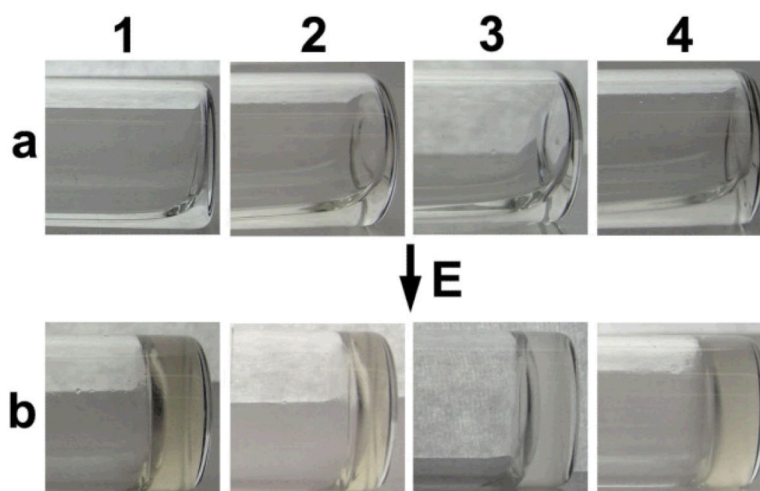


Fig. 1. Optical images of the solutions of the precursors and the corresponding hydrogels. After being dissolved in PBS buffer (pH = 7.4), the precursors (**1a**, **2a**, and **4a** at 1.0 wt %; **3a** at 0.5 wt %), upon the addition of ALP (12.5 U/mL), turn into their corresponding hydrogelators (**1b**, **2b**, **3b**, and **4b**) to result in the hydrogels. E is an alkaline phosphatase.

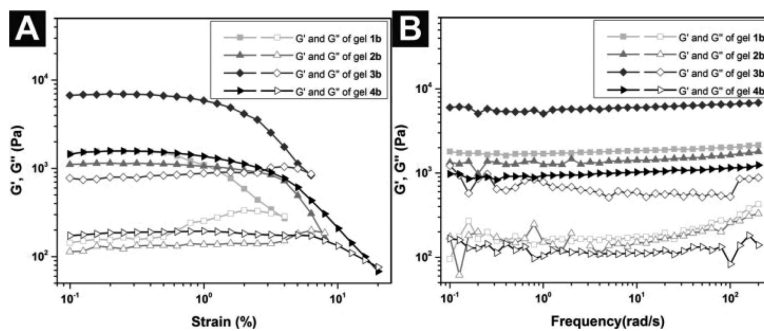


Fig. 2. (A) Strain sweep and (B) frequency sweep of the gels of **1b**, **2b**, **3b**, and **4b** at the concentration of 1.0 wt%.

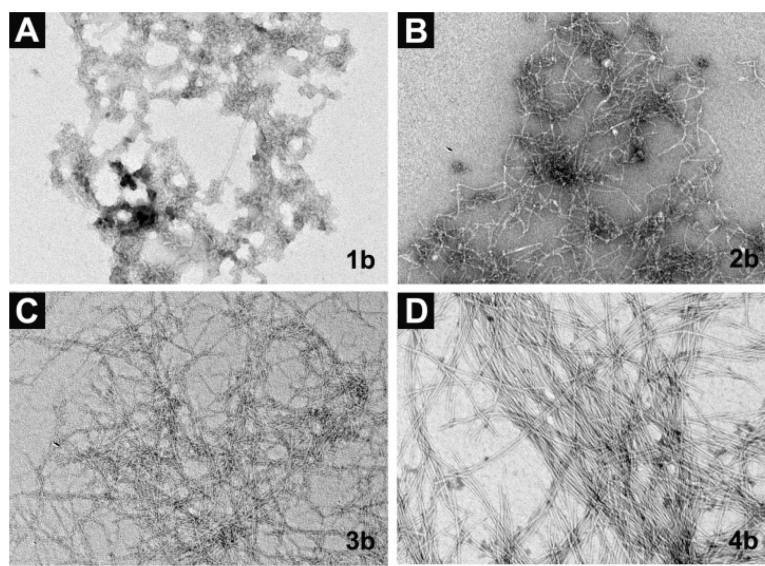


Fig. 3. Transmission electron micrograph (TEM) images of (A) gel of **1b**, (B) gel of **2b**, (C) gel of **3b**, (D) gel of **4b** shown in Fig. 1. Scale bar = 100 nm.

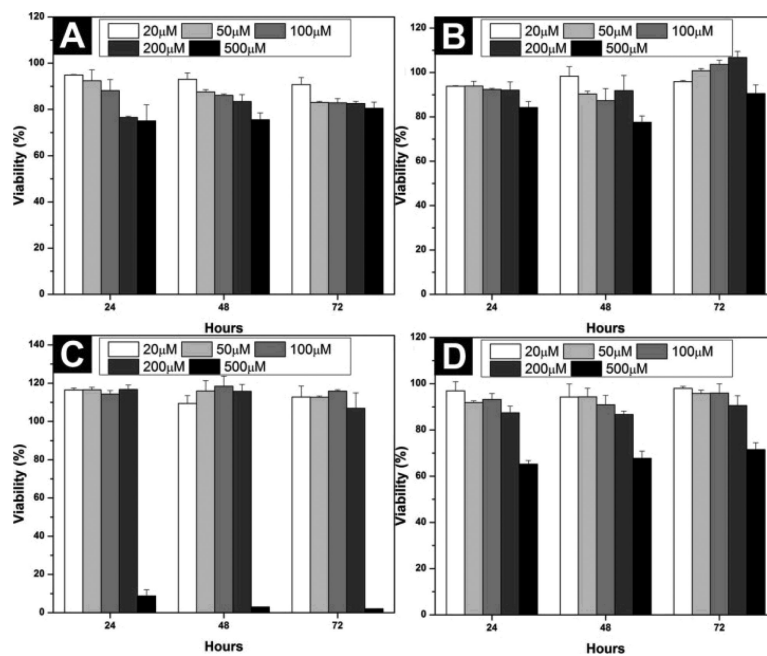


Fig. 4. Cell viability test of (A) **1a**, (B) **2a**, (C) **3a**, (D) **4a** against HeLa cells for 72 hours.